https://doi.org/10.5194/essd-2019-254
Preprint. Discussion started: 3 March 2020

Open Access Earth System Science Data Discussions

The HadGEM3-GA7.1 radiative kernel: the importance of a well-resolved stratosphere

Christopher J. Smith[1], Ryan J. Kramer[2], and Adriana Sima[3]

[1]School of Earth and Environment, University of Leeds, Leeds LS2 9JT, United Kingdom
[2]NASA Goddard Space Flight Centre, Greenbelt, MD 20771, USA
[3]Laboratoire de Météorologie Dynamique, Institut Pierre-Simon Laplace, Sorbonne Université / CNRS, 4 Place Jussieu, 75252 Paris Cedex 05, France

Correspondence: C.J.Smith (c.j.smith1@leeds.ac.uk)

Abstract. We present top-of-atmosphere and surface radiative kernels based on the atmospheric component (GA7.1) of the HadGEM3 general circulation model developed by the UK Met Office. We show that the utility of radiative kernels for forcing adjustments in idealised CO_2 perturbation experiments is most appropriate where there is sufficiently high resolution in the stratosphere in both the target climate model and the radiative kernel. This is because stratospheric cooling to a CO_2 perturbation continues to increase with height, and low-resolution or low-top kernels or climate model output are unable to fully resolve the full stratospheric temperature adjustment. In the sixth phase of the Coupled Model Intercomparison Project (CMIP6), standard atmospheric model data is available up to 1 hPa on 19 pressure levels, which is a substantial advantage compared to CMIP5. We show in the IPSL-CM6A-LR model where a full set of climate diagnostics are available that the HadGEM3-GA7.1 kernel exhibits linear behaviour and the residual error term is small. From kernels available in the literature we recommend three sets of kernels for adjustment calculations to CO_2 and well-mixed greenhouse gas perturbations based on their stratospheric resolution: HadGEM3-GA7.1, ECMWF-Oslo, and ECHAM6. The HadGEM3-GA7.1 radiative kernels are available at https://doi.org/10.5281/zenodo.3594673 (Smith, 2019).

1 Introduction

Radiative kernels describe how a small change in an atmospheric state variable affects the Earth's energy balance (Soden et al., 2008; Shell et al., 2008). They allow an analysis of climate feedbacks (Shell et al., 2008; Soden et al., 2008; Sanderson and Shell, 2012; Jonko et al., 2012; Block and Mauritsen, 2013; Huang, 2013) or forcing adjustments (Vial et al., 2013; Chung and Soden, 2015b; Smith et al., 2018; Myhre et al., 2018; Smith et al., submitted) from standardised climate model diagnostics such as those from the Coupled Model Intercomparison Projects (CMIPs). The use of radiative kernels is efficient, removing the need for time- and memory-consuming calculations of climate feedbacks online through partial radiative perturbation

https://doi.org/10.5194/essd-2019-254
Preprint. Discussion started: 3 March 2020

Open Access Earth System Science Data Discussions

calculations (Wetherald and Manabe, 1988) or offline using a standalone version of the model radiative transfer code (Colman and McAvaney, 2011).

A radiative kernel K_X is in effect a four-dimensional (time, height, latitude, longitude) array of partial differential equations describing how radiation fluxes R change with an atmospheric state variable X

$$K_X(t,z,y,x) = \left.\frac{\partial R}{\partial X}\right|_{(t,z,y,x)}. \tag{1}$$

R may be upwelling, downwelling or net, shortwave or longwave, radiation changes at any atmospheric level. Most commonly net top-of-atmosphere (TOA), surface and tropopause-level fluxes are of greatest interest. X here represents atmospheric temperature (T_a), surface (skin) temperature (T_s), water vapour (q) and surface albedo (α). For determining adjustments to a radiative forcing A_X, the kernel K_X is multiplied by the change in atmospheric state variable ΔX between two integrations of a climate model such that

$$A_X = K_X \Delta X. \tag{2}$$

ΔX is calculated as the difference of two atmosphere-only climate mode integrations using climatological sea-surface temperatures and sea ice distributions, one of which is driven by a forcing perturbation (e.g. a quadrupling of CO_2) and the other a control. For temperature and albedo the adjustment is linear with ΔX, and logarithmic for water vapour (Sanderson and Shell (2012) and Smith et al. (2018, Supplementary Material) describe how the adjustment to water vapour is applied in practice). For determining climate feedbacks λ_X, the perturbation is normalised by the change in global mean near-surface air temperature T such that

$$\lambda_X = K_X \frac{\partial X}{\partial T}. \tag{3}$$

The individual contributions from each feedback component λ_X contribute the total climate feedback $\lambda = \lambda_{T_a} + \lambda_{T_s} + \lambda_q + \lambda_\alpha + \lambda_c$ where c represents cloud feedback in the forcing-feedback representation of the Earth's energy budget $\Delta N = F - \lambda \Delta T$. Here, ΔN is the Earth's energy imbalance and F the effective radiative forcing. Likewise, the effective radiative forcing can be decomposed into

$$F = F_i + A_{T_a} + A_{T_s} + A_q + A_\alpha + A_c \tag{4}$$

with F_i being the instantaneous radiative forcing.

Usage of radiative kernels assumes that radiative perturbations change linearly with changes in atmospheric state. Where perturbations are small, linearity is an appropriate assumption both for feedbacks (Jonko et al., 2012) and adjustments (Smith et al., 2018).

Cloud adjustments and feedbacks cannot be determined using standard kernels. They may be diagnosed using the cloud kernel based on ISCCP simulator diagnostics (Zelinka et al., 2012) or from the residual of all-sky and clear-sky radiative kernels (Soden et al., 2008; Shell et al., 2008). For adjustments this calculation is

$$A_c = (F - F^{\mathrm{clr}}) - (F_i - F_i^{\mathrm{clr}}) - \sum_{X \in \{T_a, T_s, q, \alpha\}} (A_X - A_X^{\mathrm{clr}}) \tag{5}$$

https://doi.org/10.5194/essd-2019-254
Preprint. Discussion started: 3 March 2020


Open Access Earth System Science Data Discussions

where the clr superscript represents fluxes calculated in the absence of clouds. In eq. (5), the instantaneous radiative forcing must be known or estimated. This method is commonly used, requiring the production of all-sky and clear-sky kernel sets to calculate all-sky and clear-sky adjustments.

This paper introduces the top-of-atmosphere and surface radiative kernels from the HadGEM3-GA7.1 model. For stratospheric temperature adjustments we compare the radiative kernel to other kernels in the literature using available $4\times CO_2$ results from climate models contributing to the Radiative Forcing Model Intercomparison Project (RFMIP). We find that only kernels based upon climate models with a high stratospheric resolution can adequately resolve the adjustment to a CO_2 forcing.

2 Methods

One year of a pre-industrial, atmosphere-only (i.e. with climatological sea-surface temperatures and sea ice distributions) integration of the HadGEM3-GA7.1 general circulation model (Williams et al., 2018; Mulcahy et al., 2018) was run. HadGEM3-GA7.1 is the atmospheric component of the HadGEM3-GC3.1 physcial model and UKESM1.0 Earth System model that represents the UK research community's contribution to CMIP6. The model was run at LL (N96) resolution with a latitude-longitude grid of 1.25° by 1.875° and 85 vertical levels extending up to 85 km (approximately 0.005 hPa) and a native model timestep of 20 minutes.

Model diagnostics of air temperature, specific humidity, surface (skin) temperature, surface albedo (ratio of broadband upwelling to downwelling shortwave surface radiation), model level pressure, surface pressure, cloud fraction, cloud water content, cloud ice content, effective solar zenith angle and gridbox daylight fraction every two model hours were saved. These model outputs were transplanted into an offline version of the SOCRATES radiative transfer code (version 17.03; Manners et al. (2015); Edwards and Slingo (1996)) and top-of-atmosphere and surface radiative fluxes calculated for each two-hour timestep in both the shortwave and longwave spectra, for all-sky and clear-sky. SOCRATES is a broadband radiation code that uses 6 bands in the shortwave and 9 bands in the longwave and is the same radiation scheme used in the online version of HadGEM3-GC3.1 and UKESM1.0. Aerosols were neglected and greenhouse gases, including the prescribed CMIP6 monthly climatology in ozone concentrations, were set to their pre-industrial (1850) values. Following the protocol for RFMIP (Pincus et al., 2016), sea-surface temperatures and sea-ice distributions from 50 years of the HadGEM3-GC3.1 coupled model were used to build the climatology (Andrews et al., 2019).

To build the kernel, each vertical level of the model on each 2-hour timestep was perturbed separately, firstly by 1 K for air temperature, and secondly by a perturbation in specific humidity that maintains relative humidity for an increase in 1 K (without actually changing the layer temperature). The surface temperature and surface albedo were also perturbed by 1 K and 1% (additive) individually each timestep. For each perturbation, surface and TOA fluxes are again saved for clear-sky and all-sky in the shortwave (SW) and longwave (LW), and the difference compared to the control simulation gives the radiative kernel for each model level or surface. Building the kernels took in total approximately three months of computing time on 24 processors on the University of Leeds "cluj" Linux cluster.

https://doi.org/10.5194/essd-2019-254
Preprint. Discussion started: 3 March 2020

Following this, the air temperature and water vapour kernel outputs were normalised by multiplying by $10000/p_{\mathrm{thick}}$ where p_{thick} is the thickness of each level in pressure co-ordinates. This allows the 85-level native model kernel to be reduced down to the 19-level standard CMIP6 pressure levels by providing a weighted average contribution to each pressure level. The kernels are further averaged by month. In the 19-level format they can be used with standard "Amon" model output from any CMIP6 model, which is one of the key advantages of radiative kernels.

3 Kernel results

3.1 Top-of-atmosphere kernels

Figure 1 shows the TOA radiative kernels for HadGEM3-GA7.1 for clear-sky and all-sky. The air temperature, all-sky kernel (fig. 1a) shows a peak in cooling in the tropical upper troposphere, showing the importance of this region for changes in radiative balance. There are also substantial contributions to the TOA radiation balance from the lower troposphere in the mid-latitudes. For clear-sky (fig. 1b) there is more latitude-height homogeneity in the troposphere, showing the impact of removing clouds. A key feature of the air temperature kernels is the increasing strength of the LW outgoing radiation with increasing stratospheric height. The temperature kernel is negative throughout the atmosphere, in keeping with the fact that an increase in temperature results in additional Planck emission of LW radiation to space.

Water vapour kernels (fig. 1c,d) also show a peak in the upper tropical troposphere, which is opposite in sign to the negative temperature adjustment owing to the fact that water vapour is a significant greenhouse gas. In contrast to the temperature kernel, the water vapour kernel is very insensitive in the dry upper stratosphere.

The impact of cloud masking is more easily seen for the surface temperature kernels (fig. 1e,f) and surface albedo kernels (fig. 1g,h).

3.2 Surface kernels

Surface kernels are most useful for determining precipitation adjustments (Myhre et al., 2018) and feedbacks (Previdi, 2010), where the precipitation adjustment is proportional to the atmospheric absorption, calculated as the difference in TOA and surface adjustments. Figure 2 shows the surface radiative kernels for HadGEM3-GA7.1 for clear-sky and all-sky. Both the air temperature (fig. 2a,b) and water vapour (fig. 2c,d) kernels are more sensitive for perturbations close to the surface than higher in the atmosphere (note non-linear colour scales). Cloud masking for the surface temperature kernel has less of an effect for surface fluxes than for TOA fluxes (fig. 2e,f), whereas the surface albedo kernel shows quite a similar spatial pattern (fig. 2g,h) to its the TOA counterpart.

4 Comparison to other kernels for stratospheric temperature

The construction of the HadGEM3-GA7.1 kernel was motivated by the observation that adjustments to a doubling of CO_2 in PDRMIP models (Myhre et al., 2017) was around 0.3 W m^{-2} larger using the ECMWF-Oslo kernel (Myhre et al., 2018) than

https://doi.org/10.5194/essd-2019-254
Preprint. Discussion started: 3 March 2020

Open Access Earth System Science Data Discussions

Table 1. Radiative kernels considered in this study

Base model	Native model vertical levels	Top level (hPa)	3rd level (hPa)	Reference
BMRC	17	8.75	53.63	Soden et al. (2008)
CCSM4	17	10	30	Shell et al. (2008)
CESM	30	3.64	14.36	Pendergrass et al. (2018)
ECHAM5	19	10	50.39	Previdi (2010)
ECHAM6	47	0.0099	0.11	Block and Mauritsen (2013)
ECMWF-Oslo	60	0.11	0.5	Myhre et al. (2018)
GFDL	25	3.32	53.63	Soden et al. (2008)
HadGEM2	38	2.99	13.02	Smith et al. (2018)
HadGEM3-GA7.1	85	0.005	0.03	this study

other kernels used in the same study (Smith et al., 2018, Supplementary Figure 3). The ECMWF-Oslo kernel was built from ECMWF-Interim reanalysis data (Dee et al., 2011) which has 60 vertical levels up to 0.1 hPa. In contrast, most other kernels used in Smith et al. (2018) had a model top much lower.

Figure 3 shows the air temperature kernel for the stratosphere and upper troposphere for a selection of kernels available in the literature (table 1). In all cases, radiative kernels have been interpolated from their native vertical resolution (except for CCSM4, which is available only on the standard 17 CMIP5 pressure levels) to the 19 CMIP6 pressure levels for consistency with CMIP6 model output. For our calculations of stratospheric temperature adjustment, where kernels do not extend up to the 1 hPa top level of CMIP6 model output, kernels have been extended upwards using the value from the highest level where data does exist, but in fig. 3 missing data has been masked out. This extending upwards of the top level has been applied previously in adjustment calculations where the top level of the climate model is higher than the top level of the kernel (e.g. in Smith et al. (2018)). However, extending the top level of a radiative kernel upwards cannot make up for the fact that more radiation is emitted to space from the upper stratosphere for each additional K of temperature change. For kernels built from climate models with a low model top or a coarse model resolution in the stratosphere, this additional upper stratospheric cooling is missed. In fig. 3, it can be seen that the kernels based on a high-top atmospheric model with a high number of native model levels—ECHAM6, ECMWF-Oslo and HadGEM3-GA7.1—have a marked increase in both the magnitude and the rate of negative LW outgoing flux at the 5 hPa and 1 hPa levels.

The consequences for a CO_2-induced stratospheric cooling are such that the additional stratospheric adjustment from greater cooling high in the stratosphere is not accounted for with either kernels or models that are truncated too low. Figure 4 shows the atmospheric temperature anomalies simulated in atmosphere-only simulations from CMIP6 models participating in RFMIP-ERF Tier 1 experiments (Pincus et al., 2016) for a 30-year time slice simulation where CO_2 concentrations are quadrupled relative to a pre-industrial control. Stratospheric cooling continues to increase above 5 hPa in 12 out of the 13 models where data is available, with the only exception being GFDL-CM4 which has a layer of missing data at 1 hPa. Standard CMIP6

https://doi.org/10.5194/essd-2019-254
Preprint. Discussion started: 3 March 2020


Open Access Earth System Science Data Discussions

diagnostics call for model output on 19 pressure levels: 1000, 925, 850, 700, 600, 500, 400, 300, 250, 200, 150, 100, 70, 50, 30, 20, 10, 5 and 1 hPa, whereas in CMIP5 the standard set of 17 pressure levels did not include 5 and 1 hPa. Therefore, CMIP5 models were missing important additional stratospheric cooling where kernels were used for adjustment calculations.

The truncation of stratospheric height in "low top" radiative kernels (all but ECHAM6, ECMWF-Oslo and HadGEM3-GA7.1 as seen in fig. 3) has substantial consequences for adjustments to a CO_2 forcing. Figure 5 shows the stratospheric temperature adjustment to $4\times CO_2$ in the 13 models contributing to RFMIP. A simplified tropopause definition is used here, borrowed from Soden et al. (2008), of a linear in latitude ramp from 100 hPa at the equator to 300 hPa at the poles. There is a spread of around 1 W m^{-2} in calculated stratospheric temperature adjustment for each model using the full range of kernels, which is about 13% of the effective radiative forcing (ERF) for a quadrupling of CO_2 from these models (Smith et al., submitted). It can be seen in fig. 5 that the kernel estimates for stratospheric adjustment to CO_2 forcing are clustered into two groups for most models. The "low-top" radiative kernels, with the exception of GFDL and ECHAM5, produce substantially lower estimates of the stratospheric temperature adjustment than the 'high-top" kernels (HadGEM3-GA7.1, ECHAM6 and ECMWF-Oslo). The GFDL kernel has a similar magnitude and gradient of cooling between 10 and 5 hPa as the high-top kernels, and ECHAM5 has more cooling around the 100 hPa level than any other kernel. These reasons may explain why the stratospheric adjustments estimated from this kernel are more in line with the three high-top kernels. The one model where kernel estimates are not clearly separated into high and low clusters is again the GFDL-CM4 model, for which the missing data at 1 hPa impacts adjustment estimates from different kernels.

5 Accuracy of the HadGEM3-GA7.1 kernel

Where "double calls" or other methods of determining the IRF are not obtained directly from climate output, the IRF is estimated as a residual of the ERF and all adjustments. If the cloud adjustments are known (e.g. from the ISCCP simulator kernel, Zelinka et al. (2012)), it follows from eq. (4) that

$$F_i = F - A_{T_a} - A_{T_s} - A_q - A_\alpha - A_c. \tag{6}$$

The IRF is an important and useful concept in itself, as although it is not the best predictor of long-term near-surface global mean temperature changes from a forcing (Hansen et al., 2005), it can be used to benchmark the performance of radiative transfer parameterisation in climate models (Pincus et al., 2015; Soden et al., 2018).

These breakdowns of ERF into IRF and adjustments using kernels depend on the kernels being able to perform this decomposition linearly. The *residual*, ϵ, describes any error term resulting from a non-linear decomposition. Two different ways of calculating the residual can be obtained. If the all-sky IRF (e.g. from double call) and the cloud adjustment (e.g. from the ISCCP simulator kernel) are both known, then the all-sky residual ϵ_{all} is

$$\epsilon_{\text{all}} = F - F_i - A_{T_a} - A_{T_s} - A_q - A_\alpha - A_c. \tag{7}$$

If the clear-sky IRF is known, the clear-sky residual term ϵ_{clr} can be calculated as

$$\epsilon_{\text{clr}} = F^{\text{clr}} - F_i^{\text{clr}} - A_{T_a}^{\text{clr}} - A_{T_s}^{\text{clr}} - A_q^{\text{clr}} - A_\alpha^{\text{clr}}. \tag{8}$$

https://doi.org/10.5194/essd-2019-254
Preprint. Discussion started: 3 March 2020

Open Access Earth System Science Data Discussions

Table 2. IPSL-CM6A-LR double call results for 4×CO_2 experiments. IRFs are given in W m^{-2}.

Base climatology	Second call	IRF LW	IRF SW	IRF Net	IRF LW CS	IRF SW CS	IRF Net CS
pre-industrial	4×CO_2	3.66	0.83	4.49	5.02	0.46	5.48
4×CO_2	pre-industrial	4.94	0.81	5.75	6.26	0.46	6.72
Mean	Mean	4.30	0.82	5.12	5.64	0.46	6.10

Table 3. IPSL-CM6A-LR forcing and adjustments for the 4×CO_2 experiment using the HadGEM3-GA7.1 kernel. Fluxes are given in W m^{-2}. A_{T_a} strat. and A_{T_a} trop. are stratospheric and tropospheric temperature adjustments.

	ERF	IRF	A_{T_a} strat.	A_{T_a} trop.	A_{T_s}	A_q	A_α	A_c (eq. (5))	A_c (ISCCP kernel)	ϵ_{clr}	ϵ_{all}
LW	5.33	4.31	2.74	−1.38	−0.49	0.52		−0.66	−0.75	0.28	0.38
SW	2.68	0.82				0.11	0.18	1.60	1.81	−0.02	−0.23
Net	8.01	5.12	2.74	−1.38	−0.49	0.63	0.18	0.94	1.06	0.26	0.15

In practice, the kernel method is assumed to perform sufficiently well for ϵ_{clr} being within 10% of the ERF. In some circumstances, IRF is known to be identically zero (e.g. in the LW to a change in the solar constant; Smith et al. (2018)) and eq. (5) can be used with $F_i = F_i^{\mathrm{clr}} = 0$ to determine cloud adjustments.

We can test the linear separation in the IPSL-CM6A-LR model, where IRF were archived using a double call. For the RFMIP piClim-4xCO2 experiment (30-year time-slice atmosphere-only run with quadrupled CO_2) the second radiation call used a pre-industrial CO_2 concentration, and in piClim-control (pre-industrial atmosphere only run) the second radiation call saw 4×CO_2. The IRF estimated shows a substantial dependence on the base climatology, with the 4×CO_2 climate and pre-industrial second radiation call showing LW fluxes more than 1.2 W m^{-2} greater than the pre-industrial climate with 4×CO_2 second radiation call. We take the mean of the two simulations to the be the IRF.

Table 3 shows ERF, IRF, adjustments and residuals using the HadGEM3-GA7.1 radiative kernel with the IPSL-CM6A-LR model output. ISCCP simulator diagnostics are also available for this model. We therefore obtain estimates of SW and LW cloud adjustments from the ISCCP simulator kernel and use these estimates along with the IRF to estimate ϵ_{all}, alongside the cloud-masking estimate of cloud adjustment from eq. (5). For LW forcing the residuals are 0.28 W m^{-2} for ϵ_{clr} and 0.38 W m^{-2} for ϵ_{all}. Residuals are present possibly due to a slight breakdown in the linearity assumption for a forcing as large as 4×CO_2 (Jonko et al., 2012), however, the residuals are comfortably within the 10% linearity guideline. SW residuals are also within 10% of the ERF, with ϵ_{clr} being particularly small. For the net fluxes, forcings add but residuals partly cancel, such that ϵ_{clr} and ϵ_{all} are 3.2% and 1.9% of the ERF respectively.

The stratospheric temperature adjustment is the only adjustment estimate that varies significantly between radiative kernels (Smith et al., 2018). If a low-top kernel was used to estimate A_{T_a} strat. in table 3, this adjustment would be smaller, and the overall residuals for LW and net forcings larger. From fig. 5 it can be seen that some kernels produce a stratospheric temperature

https://doi.org/10.5194/essd-2019-254
Preprint. Discussion started: 3 March 2020

adjustment around 0.7 W m^{-2} lower than the HadGEM3-GA7.1 kernel, leading to residuals of the order 1 W m^{-2} or more than 10% of the ERF.

6 Conclusions

This paper serves two purposes—it introduces the radiative kernel based on the high-top HadGEM3-GA7.1 general circulation model, and it compares estimates of the the stratospheric temperature adjustment obtained with a variety of different radiative kernels for quadrupled CO_2 experiments. The HadGEM3-GA7.1 kernel is the first to our knowledge that has been produced using a CMIP6 era model, with a focus on the 19 pressure level diagnostics available in CMIP6 output. Radiative kernels are produced for both top-of-atmosphere and surface fluxes and are available on the native 85-level hybrid height grid in addition to the 19 CMIP6 pressure levels.

We show that there is a significant diversity, of about 1 W m^{-2} or 13% of the ERF for a quadrupling of CO_2, for estimates of stratospheric temperature adjustments to CO_2 depending on the radiative kernel used to derive the estimate. As tropospheric and land surface adjustments vary little between kernels to a variety of different forcing agents (Smith et al., 2018, submitted), these differences in stratospheric temperature adjustments lead to differing estimates of the total adjustment, and also of the IRF if it is calculated as a residual (Chung and Soden, 2015b, a; Soden et al., 2018). Climate feedbacks are little affected by the choice of kernel, due to the fact that stratospheric temperatures readjust quickly to an imposed forcing in coupled model simulations (Chung and Soden, 2015b).

While only one model (IPSL-CM6A-LR) archived IRF from a double call and a rigorous multi-model test is not possible, we show that the HadGEM3-GA7.1 kernel diagnoses IRF and adjustments with a small residual owing to the increased stratospheric resolution available compared to many CMIP3- and CMIP5-era kernels. We recommend that stratospheric temperature adjustments are calculated using our kernel, or the ECHAM6 (Block and Mauritsen, 2013) or ECMWF-Oslo kernels (Myhre et al., 2018). Archiving instantaneous radiative forcing from more models would be beneficial to further test the linearity assumption of the radiative kernel method.

Data availability. The HadGEM3-GA7.1 radiative kernels are available at https://doi.org/10.5281/zenodo.3594673 (Smith, 2019).

Author contributions. C.J.S. produced the HadGEM3-GA7.1 radiative kernel and led the writing of the manuscript. R.K. provided calculations of stratospheric adjustment to $4\times CO_2$ for all kernels considered in this paper. A.S. provided double call results from the IPSL-CM6A-LR model.

Competing interests. The authors declare no competing interests.

https://doi.org/10.5194/essd-2019-254
Preprint. Discussion started: 3 March 2020

Open Access Earth System Science Data Discussions

Acknowledgements. C.J.S. was supported by the European Union's Horizon 2020 research and innovation programme under grant agreement No 820829 (CONSTRAIN project). R.J.K. is supported by an appointment to the NASA Postdoctoral Program at NASA Goddard Space Flight Center. This work used the ARCHER UK National Supercomputing Service (http://www.archer.ac.uk).

https://doi.org/10.5194/essd-2019-254
Preprint. Discussion started: 3 March 2020

Open Access Earth System Science Data Discussions

References

Andrews, T., Andrews, M. B., Bodas-Salcedo, A., Jones, G. S., Kuhlbrodt, T., Manners, J., Menary, M. B., Ridley, J., Ringer, M. A., Sellar, A. A., Senior, C. A., and Tang, Y.: Forcings, Feedbacks, and Climate Sensitivity in HadGEM3-GC3.1 and UKESM1, J. Adv. Model. Earth Sy., 11, https://doi.org/10.1029/2019MS001866, 2019.

Block, K. and Mauritsen, T.: Forcing and feedback in the MPI-ESM-LR coupled model under abruptly quadrupled CO2, J. Adv. Model. Earth Sy., 5, 676–691, https://doi.org/10.1002/jame.20041, 2013.

Chung, E.-S. and Soden, B. J.: An assessment of methods for computing radiative forcing in climate models, Env. Res. Lett., 10, 074 004, https://doi.org/10.1088/1748-9326/10/7/074004, 2015a.

Chung, E.-S. and Soden, B. J.: An Assessment of Direct Radiative Forcing, Radiative Adjustments, and Radiative Feedbacks in Coupled Ocean–Atmosphere Models, J. Climate, 28, 4152–4170, https://doi.org/10.1175/JCLI-D-14-00436.1, 2015b.

Colman, R. A. and McAvaney, B. J.: On tropospheric adjustment to forcing and climate feedbacks, Clim. Dynam., 36, 1649, https://doi.org/10.1007/s00382-011-1067-4, 2011.

Dee, D. P., Uppala, S. M., Simmons, A. J., Berrisford, P., Poli, P., Kobayashi, S., Andrae, U., Balmaseda, M. A., Balsamo, G., Bauer, P., Bechtold, P., Beljaars, A. C. M., van de Berg, L., Bidlot, J., Bormann, N., Delsol, C., Dragani, R., Fuentes, M., Geer, A. J., Haimberger, L., Healy, S. B., Hersbach, H., Hólm, E. V., Isaksen, L., Kållberg, P., Köhler, M., Matricardi, M., McNally, A. P., Monge-Sanz, B. M., Morcrette, J.-J., Park, B.-K., Peubey, C., de Rosnay, P., Tavolato, C., Thépaut, J.-N., and Vitart, F.: The ERA-Interim reanalysis: configuration and performance of the data assimilation system, Q. J. R. Meteorol. Soc., 137, 553–597, https://doi.org/10.1002/qj.828, 2011.

Edwards, J. M. and Slingo, A.: Studies with a flexible new radiation code. I: Choosing a configuration for a large-scale model, Q. J. R. Meteorol. Soc., 122, 689–719, https://doi.org/10.1002/qj.49712253107, 1996.

Hansen, J., Sato, M., Ruedy, R., Nazarenko, L., Lacis, A., Schmidt, G. A., Russell, G., Aleinov, I., Bauer, M., Bauer, S., Bell, N., Cairns, B., Canuto, V., Chandler, M., Cheng, Y., Del Genio, A., Faluvegi, G., Fleming, E., Friend, A., Hall, T., Jackman, C., Kelley, M., Kiang, N., Koch, D., Lean, J., Lerner, J., Lo, K., Menon, S., Miller, R., Minnis, P., Novakov, T., Oinas, V., Perlwitz, J., Perlwitz, J., Rind, D., Romanou, A., Shindell, D., Stone, P., Sun, S., Tausnev, N., Thresher, D., Wielicki, B., Wong, T., Yao, M., and Zhang, S.: Efficacy of climate forcings, J. Geophys. Res.-Atmos., 110, https://doi.org/10.1029/2005JD005776, d18104, 2005.

Huang, Y.: On the Longwave Climate Feedbacks, J. Climate, 26, 7603–7610, https://doi.org/10.1175/JCLI-D-13-00025.1, 2013.

Jonko, A. K., Shell, K. M., Sanderson, B. M., and Danabasoglu, G.: Climate Feedbacks in CCSM3 under Changing CO2 Forcing. Part I: Adapting the Linear Radiative Kernel Technique to Feedback Calculations for a Broad Range of Forcings, J. Climate, 25, 5260–5272, https://doi.org/10.1175/JCLI-D-11-00524.1, 2012.

Manners, J., Edwards, J. M., Hill, P., and Thelen, J.: SOCRATES (Suite Of Community RAdiative Transfer codes based on Edwards and Slingo) technical guide, Tech. rep., Met Office, UK, 2015.

Mulcahy, J. P., Jones, C., Sellar, A., Johnson, B., Boutle, I. A., Jones, A., Andrews, T., Rumbold, S. T., Mollard, J., Bellouin, N., Johnson, C. E., Williams, K. D., Grosvenor, D. P., and McCoy, D. T.: Improved Aerosol Processes and Effective Radiative Forcing in HadGEM3 and UKESM1, J. Adv. Model. Earth Sy., 10, 2786–2805, https://doi.org/10.1029/2018MS001464, 2018.

Myhre, G., Forster, P., Samset, B., Hodnebrog, Sillmann, J., Aalbergsjø, S., Andrews, T., Boucher, O., Faluvegi, G., Fläschner, D., Iversen, T., Kasoar, M., Kharin, V., Kirkevag, A., Lamarque, J., Olivié, D., Richardson, T., Shindell, D., Shine, K., Stjern, C., Takemura, T., Voulgarakis, A., and Zwiers, F.: PDRMIP: A precipitation driver and response model intercomparison project-protocol and preliminary results, B. Am. Meteorol. Soc., 98, 1185–1198, https://doi.org/10.1175/BAMS-D-16-0019.1, 2017.

https://doi.org/10.5194/essd-2019-254
Preprint. Discussion started: 3 March 2020

Myhre, G., Kramer, R. J., Smith, C. J., Hodnebrog, O., Forster, P., Soden, B. J., Samset, B. H., Stjern, C. W., Andrews, T., Boucher, O., Faluvegi, G., Fläschner, D., Kasoar, M., Kirkevåg, A., Lamarque, J.-F., Olivié, D., Richardson, T., Shindell, D., Stier, P., Takemura, T., Voulgarakis, A., and Watson-Parris, D.: Quantifying the Importance of Rapid Adjustments for Global Precipitation Changes, Geophys. Res. Lett., 45, 11,399–11,405, https://doi.org/10.1029/2018GL079474, 2018.

Pendergrass, A. G., Conley, A., and Vitt, F. M.: Surface and top-of-atmosphere radiative feedback kernels for CESM-CAM5, Earth Syst. Sci. Data, 10, 317–324, https://doi.org/10.5194/essd-10-317-2018, 2018.

Pincus, R., Mlawer, E. J., Oreopoulos, L., Ackerman, A. S., Baek, S., Brath, M., Buehler, S. A., Cady-Pereira, K. E., Cole, J. N. S., Dufresne, J.-L., Kelley, M., Li, J., Manners, J., Paynter, D. J., Roehrig, R., Sekiguchi, M., and Schwarzkopf, D. M.: Radiative flux and forcing parameterization error in aerosol-free clear skies, Geophys. Res. Lett., 42, 5485–5492, https://doi.org/10.1002/2015GL064291, 2015.

Pincus, R., Forster, P. M., and Stevens, B.: The Radiative Forcing Model Intercomparison Project (RFMIP): experimental protocol for CMIP6, Geosci. Model Dev., 9, 3447–3460, https://doi.org/10.5194/gmd-9-3447-2016, https://www.geosci-model-dev.net/9/3447/2016/, 2016.

Previdi, M.: Radiative feedbacks on global precipitation, Env. Res. Lett., 5, 025 211, https://doi.org/10.1088/1748-9326/5/2/025211, 2010.

Sanderson, B. M. and Shell, K. M.: Model-Specific Radiative Kernels for Calculating Cloud and Noncloud Climate Feedbacks, J. Climate, 25, 7607–7624, https://doi.org/10.1175/JCLI-D-11-00726.1, 2012.

Shell, K. M., Kiehl, J. T., and Shields, C. A.: Using the Radiative Kernel Technique to Calculate Climate Feedbacks in NCAR's Community Atmospheric Model, J. Climate, 21, 2269–2282, https://doi.org/10.1175/2007JCLI2044.1, 2008.

Smith, C.: HadGEM3-GA7.1 radiative kernels, https://doi.org/10.5281/zenodo.3594673, 2019.

Smith, C. J., Kramer, R. J., Myhre, G., Forster, P. M., Soden, B. J., Andrews, T., Boucher, O., Faluvegi, G., Fläschner, D., Hodnebrog, O. ., Kasoar, M., Kharin, V., Kirkevåg, A., Lamarque, J.-F., Mülmenstädt, J., Olivié, D., Richardson, T., Samset, B. H., Shindell, D., Stier, P., Takemura, T., Voulgarakis, A., and Watson-Parris, D.: Understanding Rapid Adjustments to Diverse Forcing Agents, Geophys. Res. Lett., 45, 12,023–12,031, https://doi.org/10.1029/2018GL079826, 2018.

Smith, C. J., Kramer, R. J., Myhre, G., Alterskjær, K., Collins, W., Sima, A., Boucher, O., Dufresne, J.-L., Nabat, P., Michou, M., Yukimoto, S., Cole, J., Paynter, D., Shiogama, H., O'Connor, F. M., Robertson, E., Wiltshire, A., Andrews, T., Hannay, C., Miller, R., Nazarenko, L., g, A. K., Olivié, D., Fiedler, S., Pincus, R., and Forster, P. M.: Effective radiative forcing and adjustments in CMIP6 models, Atmos. Chem. Phys., submitted.

Soden, B. J., Held, I. M., Colman, R., Shell, K. M., Kiehl, J. T., and Shields, C. A.: Quantifying Climate Feedbacks Using Radiative Kernels, J. Climate, 21, 3504–3520, https://doi.org/10.1175/2007JCLI2110.1, 2008.

Soden, B. J., Collins, W. D., and Feldman, D. R.: Reducing uncertainties in climate models, Science, 361, 326–327, https://doi.org/10.1126/science.aau1864, 2018.

Vial, J., Dufresne, J.-L., and Bony, S.: On the interpretation of inter-model spread in CMIP5 climate sensitivity estimates, Clim. Dynam., 41, 3339–3362, https://doi.org/10.1007/s00382-013-1725-9, 2013.

Wetherald, R. T. and Manabe, S.: Cloud Feedback Processes in a General Circulation Model, J. Atmos. Sci., 45, 1397–1416, https://doi.org/10.1175/1520-0469(1988)045<1397:CFPIAG>2.0.CO;2, 1988.

Williams, K. D., Copsey, D., Blockley, E. W., Bodas-Salcedo, A., Calvert, D., Comer, R., Davis, P., Graham, T., Hewitt, H. T., Hill, R., Hyder, P., Ineson, S., Johns, T. C., Keen, A. B., Lee, R. W., Megann, A., Milton, S. F., Rae, J. G. L., Roberts, M. J., Scaife, A. A., Schiemann, R., Storkey, D., Thorpe, L., Watterson, I. G., Walters, D. N., West, A., Wood, R. A., Woollings, T., and Xavier, P. K.: The Met Office Global Coupled Model 3.0 and 3.1 (GC3.0 and GC3.1) Configurations, J. Adv. Model. Earth Sy., 10, 357–380, https://doi.org/10.1002/2017MS001115, 2018.

https://doi.org/10.5194/essd-2019-254
Preprint. Discussion started: 3 March 2020

Zelinka, M. D., Klein, S. A., and Hartmann, D. L.: Computing and Partitioning Cloud Feedbacks Using Cloud Property Histograms. Part I: Cloud Radiative Kernels, J. Climate, 25, 3715–3735, https://doi.org/10.1175/JCLI-D-11-00248.1, 2012.

https://doi.org/10.5194/essd-2019-254
Preprint. Discussion started: 3 March 2020

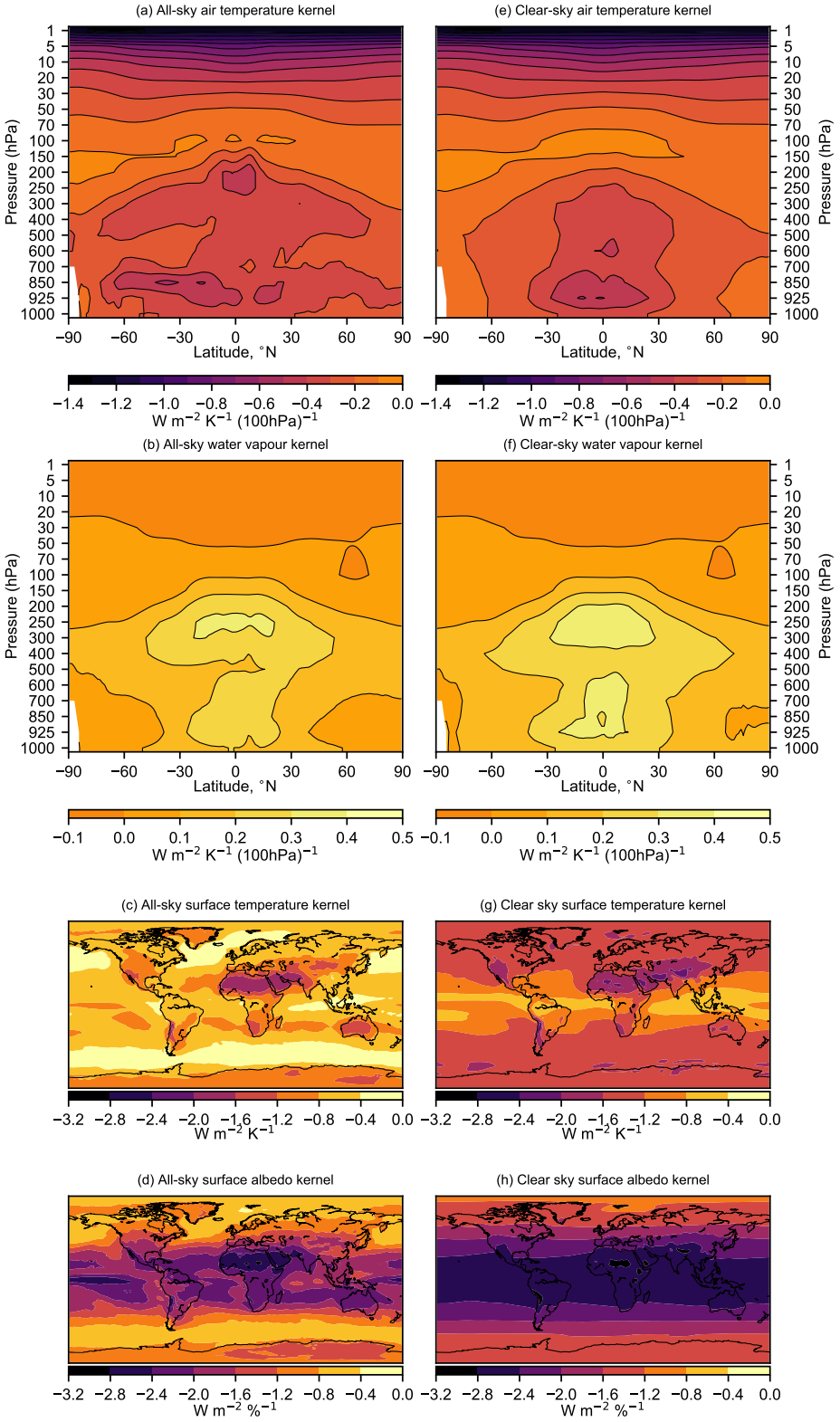

Figure 1. Top-of-atmosphere radiative kernels from HadGEM3-GA7.1.

https://doi.org/10.5194/essd-2019-254
Preprint. Discussion started: 3 March 2020

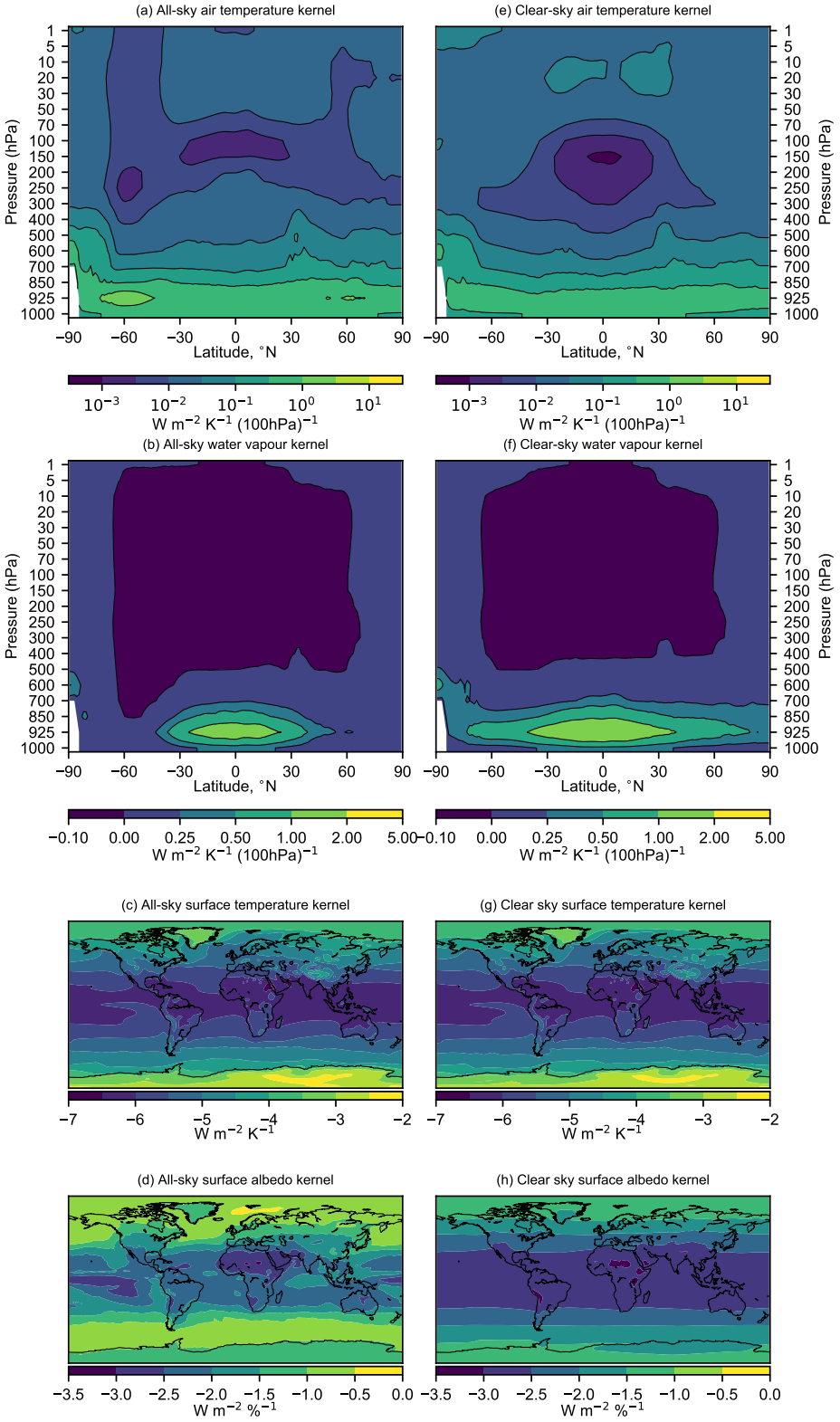

Figure 2. Surface radiative kernels from HadGEM3-GA7.1.

https://doi.org/10.5194/essd-2019-254
Preprint. Discussion started: 3 March 2020

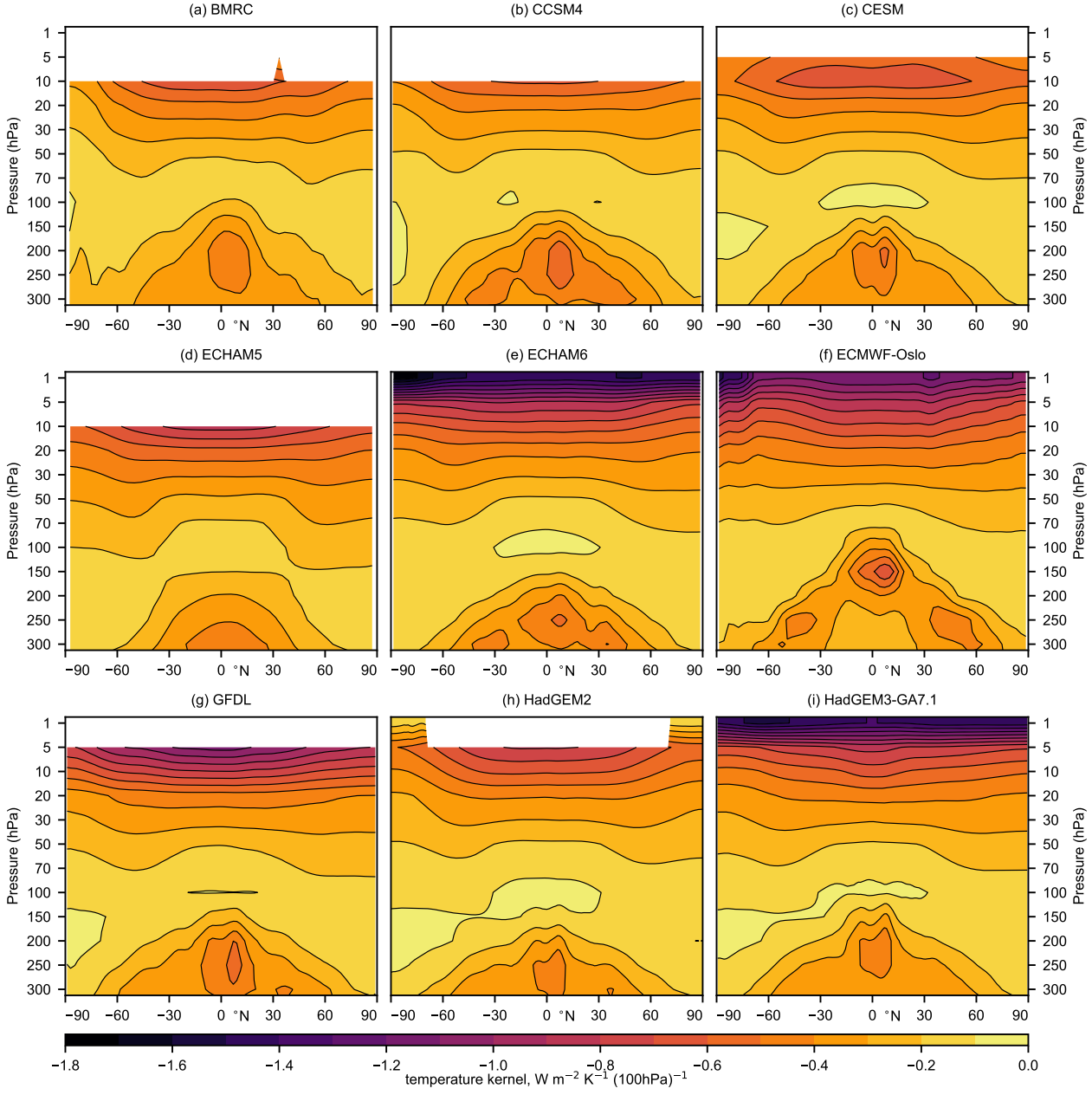

Figure 3. Air temperature radiative kernels available in the literature, truncated at 300 hPa to show the stratospheric temperature contribution. Blank areas are above the top level of the kernel.

https://doi.org/10.5194/essd-2019-254
Preprint. Discussion started: 3 March 2020

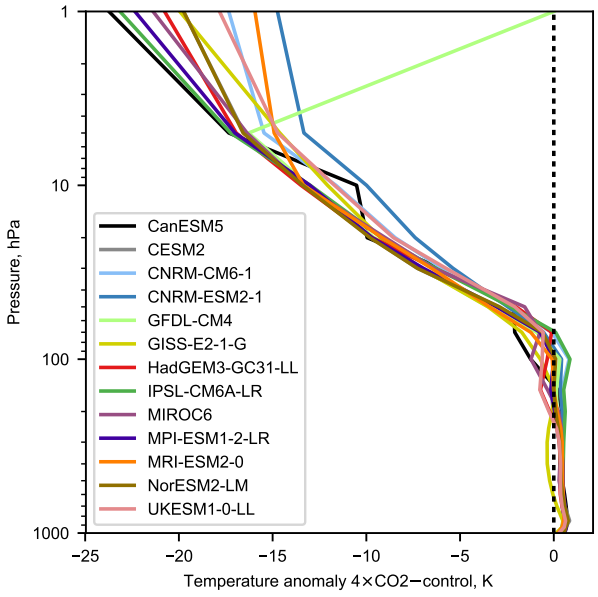

Figure 4. Atmospheric temperature differences for RFMIP models for the piClim-4xCO2 experiment minus piClim-control.

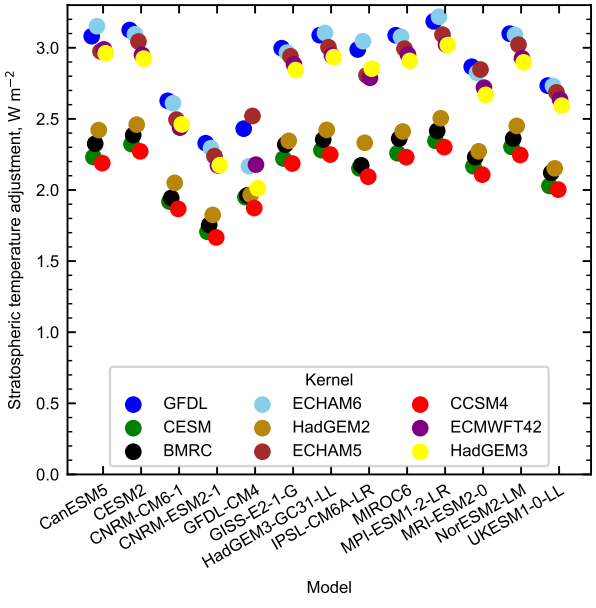

Figure 5. Stratospheric temperature adjustments calculated from RFMIP piClim-4xCO2 experiments using all kernels available in this study.